New Platinum–Iron Carbonyl Cluster Complexes and Their Reactions With Alkynes

Richard D. Adams,* Isam Arafa, Gong Chen, Jau-Ching Lii, and Jin-Guu Wang

Department of Chemistry, University of South Carolina, Columbia, South Carolina 29208

Received February 22, 1990

The reaction of $Pt(COD)_2$ with $Fe(CO)_5$ has yielded the new compounds $Pt_3Fe_3(CO)_{15}$ (1; 9%), $Pt_5Fe_2(CO)_{12}(COD)_2$ (2; 40%), and the known compound $PtFe_2(CO)_8(COD)$ (3; 3%). Compounds 1 and 2 were characterized by single-crystal X-ray diffraction analyses. Compound 1 contains a planar "raft" cluster of metal atoms consisting of a central triangle of three platinum atoms with each Pt–Pt edge bridged by a $Fe(CO)_4$ group. 1 can be reduced chemically and electrochemically to the previously known anions $[Pt_3Fe_3(CO)_{15}]^{-,2-}$. Compound 2 consists of a tetrahedral cluster of four platinum atoms with the fifth platinum atom bridging an edge of the tetrahedron and $Fe(CO)_4$ groups bridging the Pt–Pt bonds to the edge-bridging platinum atom. Compound 2 reacts with PhC_2Ph to yield the new complex $Pt_5Fe_2(CO)_7(COD)(\mu_3\text{-}PhC_2Ph)_3(\mu\text{-}PhC_2Ph)$ (4; 36%), and it reacts with PhC_2H to yield the new complex $PtFe(CO)_3(COD)[\mu\text{-}PhCC(H)C(H)CPh]$ (5; 26%). Compound 4 contains an open cluster consisting of a central square of four platinum atoms. Three of the four edges of the square are bridged by metal atoms, one Pt plus two Fe atoms. The fourth edge contains a bridging alkyne ligand. The three remaining alkyne ligands bridge the three triangular trimetal groupings formed by the edge-bridging metal atoms and the two platinum atoms in the square that they bridge. Compound 5 contains a PhCC(H)C(H)CPh ligand formed by the head-to-head coupling of two PhC_2H molecules. This ligand bridges the mutually bonded Pt and Fe atoms in the usual σ–π fashion with the π-bonding to the Fe atom. Crystal data: for 1, space group $C2/c$, a = 15.996 (6) Å, b = 11.843 (4) Å, c = 12.796 (5) Å, β = 92.35 (3)°, Z = 4, R = 0.035, R_w = 0.041 for 1331 reflections; for 2, space group $P2_1/n$, a = 9.857 (2) Å, b = 18.802 (6) Å, c = 18.319 (3) Å, β = 91.94 (1)°, Z = 4, R = 0.036, R_w = 0.039 for 3442 reflections; for 4, space group $P2_1/n$, a = 16.514 (4) Å, b = 19.727 (3) Å, c = 21.227 (6) Å, β = 103.82 (2)°, Z = 4, R = 0.051, R_w = 0.056 for 3692 reflections; for 5, space group $P2_1/c$, a = 10.498 (5) Å, b = 15.486 (6) Å, c = 14.809 (5) Å, β = 104.15 (3)°, Z = 4, R = 0.044, R_w = 0.041 for 1365 reflections.

Introduction

Heteronuclear bimetallic cluster complexes containing platinum[1] are of great interest because of the importance of bimetallic platinum catalysts to petroleum re-forming processes.[2,3] Stone has shown that $Pt(COD)_2$ (COD = 1,5-cyclooctadiene) is an excellent reagent for the preparation of heteronuclear metal complexes containing platinum.[4,5] Recently, we have achieved success in the synthesis of new heteronuclear cluster complexes through reactions of the pentacarbonyl complexes of the iron subgroup with $Pt(COD)_2$.[6,7] In this report, the results of our investigation of the reaction of $Fe(CO)_5$ with $Pt(COD)_2$ are described. Two new compounds, $Fe_3Pt_3(CO)_{15}$ (1) and $Pt_5Fe_2(CO)_{12}(COD)_2$ (2), have been isolated and characterized.

There has been great interest in the coordination and reactivity of alkynes in polynuclear metal complexes.[8,9] These complexes are believed to serve as models for the chemisorption of small molecules on metal surfaces.[10] Thus, we have investigated the reactions of 2 with PhC≡CPh and PhC≡CH. These results are also included in this report.

Experimental Section

General Considerations. All reactions were performed under a dry nitrogen atmosphere. Reagent grade solvents were dried over molecular sieves and were deoxygenated by purging with nitrogen prior to use. $Fe(CO)_5$ was purchased from Aldrich. $Pt(COD)_2$ was prepared by the reported procedure.[11] TLC separations were performed in air on plates (0.25 mm silica gel 60 F_{245}). IR spectra were recorded on a Nicolet 5-DXB FT-IR spectrometer. ^1H NMR spectra were recorded on a Bruker AM-300 spectrometer. Elemental analyses were performed by Desert Analytics, Tucson, AZ.

Preparation of $Pt_3Fe_3(CO)_{15}$ and $Pt_5Fe_2(CO)_{12}(COD)_2$. A 1.03-g (5.28-mmol) amount of $Fe(CO)_5$ was added to a hexane solution (30 mL) containing 100 mg (0.24 mmol) of $Pt(COD)_2$. The pale yellow solution turned to dark brown immediately after the addition of $Fe(CO)_5$. The solution was stirred at room temperature for 10 min. The solvent was removed under vacuum, and the residue was chromatographed by TLC with a 3/7 CH_2Cl_2/hexane solvent mixture. This yielded the following, in order of elution: brown $Pt_3Fe_3(CO)_{15}$ (1; 9.0 mg, 9%); red $PtFe_2(CO)_8(COD)$[12] (3; 5 mg, 3%); dark brown $Pt_5Fe_2(CO)_{12}(COD)_2$ (2; 32 mg, 40%). IR (ν(CO), cm^{-1}, in hexane): for 1, 2057 (s), 2009 (m), 1999 (m); for 2, 2068 (m), 2029 (m), 2009 (s), 2003 (sh), 1962 (w).

Reaction of $Pt_3Fe_3(CO)_{15}$ with $[Bu_4N]OH$. A 0.5-mL amount of a 0.0625 M solution of $[Bu_4N]OH$ in CH_3OH (prepared from 805 mg of Bu_4NBr and 100 mg of NaOH in 40 mL of CH_3OH) was added to 3.0 mg of $Pt_3Fe_3(CO)_{15}$ (0.0025 mmol) in 2 mL of CH_3OH under nitrogen. The color of the solution changed from brown to green in a few minutes. The infrared spectrum of the green solution was essentially the same as that reported for the dianion $[Pt_3Fe_3(CO)_{15}]^{2-}$, prepared previously by another method.[13] The conversion appeared to be quantitative by IR

(1) Farrugia, L. J. *Adv. Organomet. Chem.*, in press.
(2) (a) Sinfelt, J. H. *Bimetallic Catalysts*; Wiley: New York, 1983. (b) Sinfelt, J. H. *Acc. Chem. Res.* **1977**, *10*, 15.
(3) (a) Sachtler, W. M. H. *J. Mol. Catal.* **1984**, *25*, 1. (b) Ponec, V. *Adv. Catal.* **1983**, *32*, 149.
(4) Stone, F. G. A. *Acc. Chem. Res.* **1981**, *14*, 318.
(5) Stone, F. G. A. *Inorg. Chim. Acta* **1981**, *50*, 33.
(6) Adams, R. D.; Chen, G.; Wang, J.-G. *Polyhedron* **1989**, *8*, 2521.
(7) Adams, R. D.; Chen, G.; Wang, J.-G.; Wu, W. *Organometallics* **1990**, *9*, 1339.
(8) Raithby, P. R.; Rosales, M. J. *Adv. Inorg. Chem. Radiochem.* **1985**, *29*, 169.
(9) Sappa, E.; Tiripicchio, A.; Braunstein, P. *Chem. Rev.* **1983**, *83*, 203.
(10) Muetterties, E. L.; Rhodin, T. N.; Band, E.; Brucker, C. F.; Pretzer, W. R. *Chem. Rev.* **1979**, *79*, 91.
(11) (a) Green, M.; Howard, J. A. K.; Spencer, J. L.; Stone, F. G. A. *J. Chem. Soc., Dalton Trans.* **1977**, 271. (b) Spencer, J. L. *Inorg. Synth.* **1979**, *19*, 213.
(12) Farrugia, L. J.; Howard, J. A. K.; Mitprachachon, P.; Stone, F. G. A.; Woodward, P. *J. Chem. Soc., Dalton Trans.* **1981**, 1134.

0276-7333/90/2309-2350$02.50/0

Table I. Crystallographic Data for Diffraction Studies of Compounds 1, 2, 4, and 5

	1	2	4	5
empirical formula	$Pt_3Fe_3O_{15}C_{15}$	$Pt_5Fe_2O_{12}C_{28}H_{24}$	$Pt_5Fe_2O_7C_{71}H_{52}$	$PtFeO_3C_{27}H_{24}$
fw	1172.97	1639.63	2104.33	647.42
cryst syst	monoclinic	monoclinic	monoclinic	monoclinic
lattice params				
a, Å	15.996 (6)	9.857 (2)	16.514 (4)	10.498 (5)
b, Å	11.843 (4)	18.802 (6)	19.727 (3)	15.486 (6)
c, Å	12.796 (5)	18.319 (3)	21.227 (6)	14.809 (5)
β, deg	92.35 (3)	91.94 (1)	103.82 (2)	104.15 (3)
V, Å^3	2422 (1)	3393 (2)	6715 (5)	2334 (2)
space group	$C2/c$ (No. 15)	$P2_1/n$ (No. 14)	$P2_1/n$ (No. 14)	$P2_1/c$ (No. 14)
Z	4	4	4	4
D_{calc}, g/cm^3	3.22	3.21	2.08	1.84
F_{000}	2088	2920	3736	1256
μ(Mo Kα), cm^{-1}	192.65	216.39	109.54	66.95
abs cor	analytical	analytical	analytical	empirical
transmissn coeff: max/min	0.056/0.017	0.106/0.034	0.534/0.302	[illegible]
temp (±3), °C	23	23	23	23
$2\theta_{max}$, deg	45.0	45.0	40.0	40.0
no. of observns ($I > 3\sigma(I)$)	1331	3442	3692	1365
no. of variables	165	424	376	169
residuals: R; R_w	0.035; 0.041	0.036; 0.039	0.051; 0.056	0.044; 0.041
goodness of fit indicator	2.40	1.89	2.01	1.32
max shift in final cycle	0.02	0.03	0.40	0.02
largest peak in final diff map, e/Å^3	1.56	1.12	2.20	0.87

spectroscopy. The solution was concentrated and stored at −20 °C overnight. During this time, green crystals formed. These crystals were separated, and their crystallographic unit cell was determined by X-ray diffraction and found to be the same as that reported for $[NBu_4^n]_2[Pt_3Fe_3(CO)_{15}]$.[13]

Reaction of 2 with PhC≡CPh. A 23.0-mg (0.13-mmol) amount of PhC≡CPh was added to a 15-mL hexane solution of **2** (18 mg, 0.011 mmol) at 25 °C. The solution was heated to reflux for 3 h. The solvent was removed under vacuum. The residue was extracted with a minimum amount of CH_2Cl_2 and the extract chromatographed by TLC on silica gel with a 1/4 CH_2Cl_2/hexane solvent mixture. This yielded dark brown $Pt_5Fe_2(CO)_7(PhC_2Ph)_4(C_8H_{12})$ (**4**; 8.0 mg, 36%). IR (ν(CO), cm^{-1}, in hexane): 2054 (m), 2020 (s), 2009 (vs), 1970 (w), 1963 (vw), 1955 (w), 1935 (w). ^{1}H NMR (δ, in $CDCl_3$): 6.20–7.62 (m, Ph), 4.65 (m, CH), 4.25 (m, CH), 2.45 (m, CH_2).

Reaction of 2 with PhC≡CH. In a typical reaction, 11.2 mg of PhC≡CH (0.11 mmol) was added to a solution of 18.0 mg of **2** (0.011 mmol) in 14 mL of hexane. The solution was refluxed for 3 h, cooled, concentrated, and separated by TLC with a 4/1 hexane/CH_2Cl_2 solvent mixture. The major product, yellow $PtFe(CO)_3(COD)[\mu$-PhCC(H)C(H)CPh] (**5**; 3.2 mg, 26%), was separated from 1.4 mg of unreacted **2**. IR (ν(CO), cm^{-1}, in hexane): 2031 (vs), 1972 (s), 1952 (s). ^{1}H NMR (δ, in $CDCl_3$): 7.08–7.12 (m, Ph, 10 H), 5.52 (s, CH, 2 H, J_{Pt-H} = 88 Hz), 4.67 (m, CH, 2 H), 4.26 (m, CH, 2 H), 2.41 (m, 8 H, CH_2).

Electrochemical Measurements. Cyclic voltammetry measurements were made by using a BAS100A electrochemical analyzer. Tetrabutylammonium hexafluorophosphate (0.1 M) was used as the supporting electrolyte. Solutions of **1** in CH_2Cl_2 solvent were prepared under a nitrogen atmosphere, and the electrochemical cell was purged with nitrogen prior to the measurements. The measurements were made at 25 °C by using a platinum electrode with a saturated sodium chloride calomel reference and a scan rate of 100 mV/s. In a typical run, 3.6 mg of **1** was dissolved in ~10 mL of CH_2Cl_2. The voltammogram showed two reversible one-electron-redox processes. The one centered at $E_{1/2}$ = 0.09 V, i_c/i_a = 0.91, ΔE_p = 66 mV was assigned to the 0/−1 couple. The one at $E_{1/2}$ = −0.50 V, i_c/i_a = 1.01, ΔE_p = 72 mV was assigned to the −1/−2 couple.

Crystallographic Analyses. Opaque dark brown crystals of **1** and black crystals of **2** were grown by slow evaporation of solvent from a hexane solution at −20 °C. Black crystals of **4** were grown from solution in a CH_2Cl_2/hexane solvent mixture by cooling to −20 °C. The data crystals were mounted in thin-walled glass capillaries. Diffraction measurements were made on a Rigaku AFC6S automatic diffractometer by using graphite-monochromatized Mo Kα radiation. Unit cells were determined and refined from 15 randomly selected reflections obtained by using the diffractometer automatic search, center, index, and least-squares routines. Crystal data, data collection parameters, and results of the analyses are listed in Table I. All data processing was performed on a Digital Equipment Corp. MICROVAX II computer by using the TEXSAN structure solving program library (version 2.0) obtained from Molecular Structure Corp., The Woodlands, TX. Neutral-atom scattering factors were obtained from the standard sources.[14a] Anomalous dispersion corrections were applied to all non-hydrogen atoms.[14b] Full-matrix least-squares refinements minimized the function $\sum_{hkl} w(|F_o| - |F_c|)^2$, where $w = 1/\sigma(F)^2$, $\sigma(F) = \sigma(F_o^2)/2F_o$, and $\sigma(F_o^2) = [\sigma(I_{raw})^2 + (0.02F_o^2)^2]^{1/2}/Lp$.

Compound **1** crystallized in the monoclinic crystal system. The systematic absences observed in the data were consistent with either of the space groups $C2/c$ and Cc. The space group $C2/c$ was assumed and confirmed by the successful solution and refinement of the structure. The structure was solved by a combination of direct methods (MITHRIL) and difference Fourier techniques. All atoms were refined with anisotropic thermal parameters.

Compound **2** crystallized in the monoclinic crystal system. The space group $P2_1/n$ was established from the systematic absences observed in the data. The positions of the metal atoms were determined by direct methods (MITHRIL). All other atom positions were obtained from subsequent difference Fourier syntheses. All non-hydrogen atoms were refined with anisotropic thermal parameters. Hydrogen atom positions were calculated and were included in the structure factor calculations, but they were not refined.

Compound **4** crystallized in the monoclinic crystal system. The space group $P2_1/n$ was established by the absences in the data. The structure of **4** was solved by a combination of direct methods (MITHRIL) and difference Fourier syntheses. Only the metal atoms were refined with anisotropic thermal parameters. The positions of the hydrogen atoms on the phenyl rings were calculated and were included in the structure factor calculations, but they were not refined.

Compound **5** crystallized in the monoclinic crystal system. The space group $P2_1/c$ was established from the systematic absences in the data. The structure was solved by direct methods (MITHRIL). Due to the limited amount of data that were available, only the metal atoms and carbonyl ligands were refined with anisotropic

(13) Longoni, G.; Manassero, M.; Sansoni, M. *J. Am. Chem. Soc.* **1980**, *102*, 7973.

(14) (a) *International Tables for X-ray Crystallography*; Kynoch: Birmingham, England, 1975; Vol. IV, Table 2.2B, pp 99–101. (b) *Ibid.*, Table 2.3.1, pp 149–150.

Table II. Positional Parameters and B(eq) Values for $Pt_3Fe_3(CO)_{15}$ (1)

atom	x	y	z	B(eq), Å²
Pt(1)	1.0000	0.11311 (5)	1/4	3.35 (4)
Pt(2)	1.07364 (3)	0.30279 (4)	0.29575 (4)	3.37 (3)
Fe(1)	1.0000	0.4912 (2)	1/4	3.8 (1)
Fe(2)	1.15229 (13)	0.11375 (15)	0.32243 (16)	3.8 (1)
O(11)	1.0000	−0.1396 (12)	1/4	5.9 (9)
O(21)	1.2186 (7)	0.4320 (10)	0.3955 (10)	6.6 (7)
O(31)	1.2070 (8)	−0.1193 (9)	0.3347 (11)	7.3 (8)
O(32)	1.1700 (8)	0.1507 (10)	0.0970 (10)	6.3 (7)
O(33)	1.3176 (7)	0.1932 (10)	0.3944 (11)	6.9 (7)
O(34)	1.0629 (8)	0.1156 (10)	0.5176 (10)	7.0 (7)
O(41)	0.9153 (8)	0.4399 (11)	0.4437 (9)	6.9 (7)
O(42)	1.1156 (9)	0.6624 (9)	0.3374 (10)	7.0 (7)
C(11)	1.0000	−0.0433 (17)	1/4	4 (1)
C(21)	1.1644 (10)	0.3817 (13)	0.3598 (14)	5.0 (8)
C(31)	1.1862 (9)	−0.0293 (12)	0.3284 (12)	4.5 (8)
C(32)	1.1607 (9)	0.1384 (12)	0.1845 (14)	4.6 (8)
C(33)	1.2530 (10)	0.1612 (13)	0.3686 (12)	4.6 (8)
C(34)	1.0946 (10)	0.1179 (12)	0.4429 (13)	4.8 (8)
C(41)	0.9479 (10)	0.4548 (12)	0.3683 (13)	4.6 (8)
C(42)	1.0705 (11)	0.5986 (12)	0.3029 (13)	5.1 (9)

Table III. Intramolecular Distances for 1[a]

Pt(1)–C(11)	1.85 (2)	Fe(1)–C(41)	1.81 (2)
Pt(1)–Fe(2)	2.571 (2)	Fe(1)–C(42)	1.81 (2)
Pt(1)–Pt(2)	2.592 (1)	Fe(2)–C(31)	1.78 (1)
Pt(2)–C(21)	1.89 (2)	Fe(2)–C(33)	1.78 (2)
Pt(2)–Fe(1)	2.580 (2)	Fe(2)–C(32)	1.80 (2)
Pt(2)–Fe(2)	2.584 (2)	Fe(2)–C(34)	1.83 (2)
Pt(2)–Pt(2)′	2.587 (2)	O–C (av)	1.13 (2)

[a] Distances are in angstroms. Estimated standard deviations in the least significant figure are given in parentheses.

Table IV. Intramolecular Bond Angles for 1[a]

C(11)–Pt(1)–Fe(2)	90.17 (4)	C(41)–Fe(1)–Pt(2)	80.0 (5)
C(11)–Pt(1)–Pt(2)	150.06 (2)	C(41)–Fe(1)–Pt(2)	76.2 (5)
Fe(2)–Pt(1)–Fe(2)	179.7 (1)	C(42)–Fe(1)–Pt(2)	104.5 (5)
Fe(2)–Pt(1)–Pt(2)	60.06 (5)	C(42)–Fe(1)–Pt(2)	164.4 (5)
Fe(2)–Pt(1)–Pt(2)	119.60 (5)	Pt(2)–Fe(1)–Pt(2)	60.20 (7)
Pt(2)–Pt(1)–Pt(2)	59.87 (4)	C(31)–Fe(2)–Pt(1)	107.2 (5)
C(21)–Pt(2)–Fe(1)	90.3 (4)	C(31)–Fe(2)–Pt(2)	167.5 (5)
C(21)–Pt(2)–Fe(2)	90.6 (4)	C(33)–Fe(2)–Pt(1)	161.8 (5)
C(21)–Pt(2)–Pt(2)	150.1 (4)	C(33)–Fe(2)–Pt(2)	101.5 (5)
C(21)–Pt(2)–Pt(1)	149.6 (4)	C(32)–Fe(2)–Pt(1)	75.8 (5)
Fe(1)–Pt(2)–Fe(2)	174.23 (5)	C(32)–Fe(2)–Pt(2)	77.6 (4)
Fe(1)–Pt(2)–Pt(2)	59.90 (3)	C(34)–Fe(2)–Pt(1)	78.5 (5)
Fe(1)–Pt(2)–Pt(1)	119.96 (4)	C(34)–Fe(2)–Pt(2)	80.1 (5)
Fe(2)–Pt(2)–Pt(2)	119.28 (5)	Pt(1)–Fe(2)–Pt(2)	60.39 (5)
Fe(2)–Pt(2)–Pt(1)	59.55 (5)	O–C–M (av)	177 (1)
Pt(2)–Pt(2)–Pt(1)	60.06 (2)		

[a] Angles are in degrees. Estimated standard deviations in the least significant figure are given in parentheses.

thermal parameters. Hydrogen atom positions were calculated, and their scattering was added to the structure factor calculations, but their positions were not refined.

Results and Discussion

The reaction of $Pt(COD)_2$ with $Fe(CO)_5$ in hexane solution at 25 °C has yielded the complexes $Pt_3Fe_3(CO)_{15}$ (1; 9%), $Pt_5Fe_2(CO)_{12}(COD)_2$ (2; 40%), and $PtFe_2(CO)_8(COD)$ (3; 3%). Compound 3 has been described previously.[12] Compounds 1 and 2 are new and were characterized by single-crystal X-ray diffraction analyses. Final atomic positional parameters for 1 are listed in Table II. Selected intramolecular bond distances and angles are listed in Tables III and IV. An ORTEP diagram of the molecular structure of 1 is shown in Figure 1. The molecule contains a crystallographically imposed 2-fold rotation axis that passes through the atoms Fe(1), Pt(1), C(11), and O(11). The six metal atoms are arranged in the well-known planar

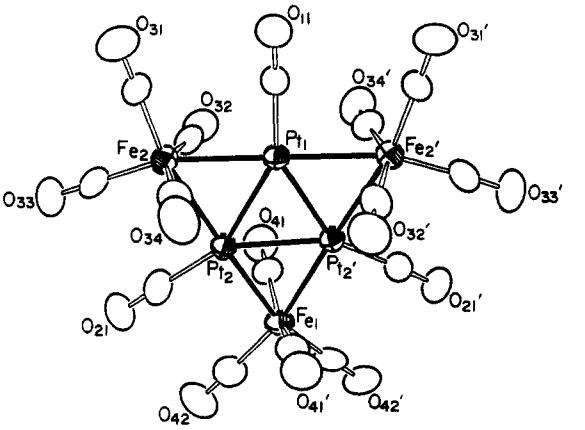

Figure 1. ORTEP drawing of $Pt_3Fe_3(CO)_{15}$ (1) showing 40% probability thermal ellipsoids.

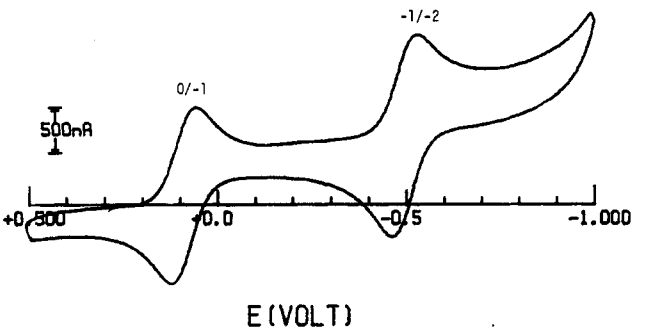

Figure 2. Cyclic voltammogram of $Pt_3Fe_3(CO)_{15}$ (1) in CH_2Cl_2 solution.

Table V. Bond Distances (Å) in 1, 1^-, and 1^{2-}

	1	1^-	1^{2-}
Pt–Pt	2.590[a]	2.656[b]	2.750[b]
Pt–Fe	2.578[c]	2.587[d]	2.596[d]

[a] Esd on single Pt–Pt distance 0.002.[13] [b] Esd on single Pt–Pt distance 0.001.[13] [c] Esd on single Pt–Fe distance 0.002.[13] [d] Esd on single Pt–Fe distance 0.004.[13]

"raft" structure. The platinum atoms form a central triangular cluster with $Fe(CO)_4$ groupings bridging each Pt–Pt edge. Each platinum atom also contains one linear terminal carbonyl ligand. Compound 1 is structurally related to the series of anions $[Pt_3Fe_3(CO)_{15}]^{-,2-}$ (1^-, 1^{2-}) that was reported by Longoni et al. in 1980.[13] All three complexes are isostructural but differ in their total number of electrons. On the basis of the significant decrease of the Pt–Pt bond lengths in going from the dianion 1^{2-} to monoanion 1^- (see Table V), Longoni concluded that the highest occupied molecular orbital was centered on the Pt_3 triangle and was antibonding in character. This is supported by an extended Hückel molecular orbital analysis that has recently been performed by Pergola et al., who showed that the HOMO in the anions was an in-plane σ antibonding orbital that is centered principally on the Pt_3 triangle.[15] This conclusion is further supported by the structure of 1, which shows that the removal of one electron from 1^- to yield 1 produces yet another significant decrease, 0.066 (2) Å, in the Pt–Pt bond lengths. In 1 the Pt_3 cluster can be assigned 42 electrons, which is the electron-precise value for a triangular trinuclear cluster of metal atoms with 16-electron configurations. The Pt–Fe distances show only a minor decrease in length as the two

(15) Pergola, R. D.; Garlaschelli, L.; Mealli, C.; Proserpio, D. M.; Zanello, P. *J. Cluster Sci.*, in press.

Table VI. Positional Parameters and B(eq) Values for $Pt_3Fe_2(CO)_{12}(C_8H_{12})_2$ (2)

atom	x	y	z	B(eq), Å²
Pt(1)	0.94314 (7)	0.22408 (4)	0.09053 (4)	2.78 (3)
Pt(2)	1.13582 (7)	0.24272 (4)	0.19233 (4)	2.60 (3)
Pt(3)	1.01847 (7)	0.35456 (4)	0.12712 (4)	3.26 (3)
Pt(4)	1.16794 (7)	0.13092 (4)	0.09553 (4)	2.71 (3)
Pt(5)	0.96027 (7)	0.12696 (4)	0.20831 (4)	3.20 (3)
Fe(1)	1.2147 (3)	0.37045 (15)	0.22340 (15)	3.8 (1)
Fe(2)	0.8218 (3)	0.33036 (16)	0.03209 (15)	3.9 (1)
O(10)	0.8017 (15)	0.1141 (8)	−0.0004 (9)	7 (1)
O(11)	1.2217 (18)	0.5247 (9)	0.2395 (10)	8 (1)
O(12)	1.3690 (17)	0.3690 (9)	0.0872 (10)	7 (1)
O(13)	0.9725 (20)	0.3551 (10)	0.3106 (10)	8 (1)
O(14)	1.432 (2)	0.3356 (11)	0.3297 (13)	10 (1)
O(21)	0.7238 (18)	0.4710 (10)	−0.0165 (11)	8 (1)
O(22)	1.0616 (15)	0.3295 (8)	−0.0578 (8)	5.9 (8)
O(23)	0.6742 (17)	0.3262 (12)	0.1697 (10)	10 (1)
O(24)	0.6395 (18)	0.2496 (11)	−0.0672 (11)	9 (1)
O(20)	1.3314 (16)	0.1742 (9)	0.2988 (9)	6 (1)
O(31)	1.0057 (19)	0.5124 (9)	0.0952 (10)	8 (1)
O(32)	1.0189 (15)	0.0027 (8)	0.1231 (8)	5.6 (8)
C(10)	0.8546 (18)	0.1563 (11)	0.0345 (10)	4 (1)
C(11)	1.220 (2)	0.4632 (12)	0.2339 (11)	5 (1)
C(12)	1.310 (2)	0.3659 (10)	0.1426 (12)	4 (1)
C(13)	1.066 (3)	0.3576 (13)	0.2747 (12)	6 (1)
C(14)	1.345 (3)	0.3503 (13)	0.2894 (16)	6 (1)
C(21)	0.765 (2)	0.4178 (13)	0.0043 (12)	5 (1)
C(22)	0.973 (2)	0.3304 (11)	−0.0215 (11)	5 (1)
C(23)	0.736 (2)	0.3294 (13)	0.1123 (13)	6 (1)
C(24)	0.708 (2)	0.2821 (13)	−0.0284 (13)	5 (1)
C(20)	1.2584 (19)	0.1994 (11)	0.2580 (11)	4 (1)
C(31)	1.009 (2)	0.4521 (11)	0.1091 (12)	5 (1)
C(41)	1.2766 (20)	0.2121 (10)	0.0161 (11)	4 (1)
C(42)	1.370 (2)	0.1965 (10)	0.0649 (12)	4 (1)
C(43)	1.4864 (18)	0.1418 (14)	0.0526 (14)	6 (1)
C(44)	1.448 (2)	0.0686 (12)	0.0824 (14)	6 (1)
C(45)	1.3028 (19)	0.0450 (10)	0.0664 (10)	4 (1)
C(46)	1.2186 (18)	0.0597 (10)	0.0074 (10)	3.4 (9)
C(47)	1.259 (2)	0.0986 (12)	−0.0593 (12)	5 (1)
C(48)	1.2468 (19)	0.1790 (10)	−0.0571 (10)	4 (1)
C(51)	0.816 (2)	0.2021 (12)	0.2731 (13)	5 (1)
C(52)	0.910 (2)	0.1822 (13)	0.3221 (12)	5 (1)
C(53)	0.897 (2)	0.1266 (17)	0.3799 (10)	7 (1)
C(54)	0.945 (3)	0.0549 (16)	0.3555 (13)	7 (2)
C(55)	0.918 (2)	0.0359 (12)	0.2784 (11)	5 (1)
C(56)	0.804 (3)	0.0512 (13)	0.2378 (13)	6 (1)
C(57)	0.680 (3)	0.088 (2)	0.2638 (15)	9 (2)
C(58)	0.678 (2)	0.171 (2)	0.2602 (16)	9 (2)
C(32)	1.0408 (18)	0.0639 (10)	0.1349 (9)	3.1 (9)

electrons are removed from the dianion.

To establish the relation of 1 to the anions prepared by Longoni, the reaction of 1 with $[NBu^n_4]OH$ was performed. This was found to produce $[NBu^n_4]_2[Pt_3Fe_3(CO)_{15}]$ in essentially a quantitative yield. The connection was further established by electrochemical methods. The cyclic voltammogram of 1 was obtained in CH_2Cl_2 solution and is shown in Figure 2. This measurement revealed two reversible one-electron-redox processes. The process centered at $E_{1/2}$ = 0.09 V is assigned to the 0/−1 redox couple, while the one at $E_{1/2}$ = −0.50 V is assigned to the −1/−2 redox couple. A similar result was obtained by Pergola et al., who studied the cyclic voltammetry of the Longoni anions.[15] These workers also isolated and spectroscopically characterized 1 by chemical oxidation of the anions.

An ORTEP drawing of the molecular structure of 2 is shown in Figure 3. Final positional parameters are listed in Table VI. Selected interatomic distances and angles are listed in Tables VII and VIII. The cluster consists of a tetrahedron of four platinum atoms with one platinum atom, Pt(3), bridging an edge of this cluster and $Fe(CO)_4$ groups bridging each of the Pt–Pt bonds between Pt(3) and the tetrahedron. The platinum atoms Pt(4) and Pt(5) each contain one COD ligand. The Pt(4)–Pt(5) bond contains a bridging carbonyl ligand, but this is still the longest metal–metal bond in the molecule, 2.958 (1) Å. The

Table VII. Intramolecular Distances for 2[a]

Pt(1)–C(10)	1.84 (2)	Pt(4)–C(41)	2.39 (2)
Pt(1)–Fe(2)	2.546 (3)	Pt(4)–C(42)	2.43 (2)
Pt(1)–Pt(2)	2.640 (1)	Pt(4)–Pt(5)	2.958 (1)
Pt(1)–Pt(3)	2.643 (1)	Pt(5)–C(32)	1.98 (2)
Pt(1)–Pt(4)	2.824 (1)	Pt(5)–C(56)	2.18 (2)
Pt(1)–Pt(5)	2.827 (1)	Pt(5)–C(55)	2.19 (2)
Pt(2)–C(20)	1.86 (2)	Pt(5)–C(51)	2.36 (2)
Pt(2)–Fe(1)	2.582 (3)	Pt(5)–C(52)	2.40 (2)
Pt(2)–Pt(3)	2.663 (1)	Fe(1)–C(11)	1.76 (2)
Pt(2)–Pt(4)	2.775 (1)	Fe(1)–C(14)	1.77 (3)
Pt(2)–Pt(5)	2.802 (1)	Fe(1)–C(12)	1.78 (2)
Pt(3)–C(31)	1.87 (2)	Fe(1)–C(13)	1.79 (2)
Pt(3)–Fe(1)	2.591 (3)	Fe(2)–C(23)	1.72 (2)
Pt(3)–Fe(2)	2.602 (3)	Fe(2)–C(24)	1.80 (3)
Pt(4)–C(32)	1.93 (2)	Fe(2)–C(21)	1.80 (2)
Pt(4)–C(46)	2.17 (2)	Fe(2)–C(22)	1.81 (2)
Pt(4)–C(45)	2.17 (2)	O–C (av)	1.15 (2)

[a] Distances are in angstroms. Estimated standard deviations in the least significant figure are given in parentheses.

Table VIII. Intramolecular Bond Angles for 2[a]

C(10)–Pt(1)–Fe(2)	95.9 (6)	C(41)–Pt(4)–Pt(2)	88.2 (5)
C(10)–Pt(1)–Pt(2)	143.4 (6)	C(41)–Pt(4)–Pt(1)	87.2 (5)
C(10)–Pt(1)–Pt(3)	155.4 (6)	C(41)–Pt(4)–Pt(5)	141.0 (4)
C(10)–Pt(1)–Pt(4)	86.8 (5)	C(42)–Pt(4)–Pt(2)	82.9 (5)
C(10)–Pt(1)–Pt(5)	89.6 (6)	C(42)–Pt(4)–Pt(1)	109.1 (5)
Fe(2)–Pt(1)–Pt(2)	120.62 (8)	C(42)–Pt(4)–Pt(5)	140.2 (5)
Fe(2)–Pt(1)–Pt(3)	60.14 (7)	Pt(2)–Pt(4)–Pt(1)	56.26 (3)
Fe(2)–Pt(1)–Pt(4)	149.04 (7)	Pt(2)–Pt(4)–Pt(5)	58.41 (2)
Fe(2)–Pt(1)–Pt(5)	147.43 (7)	Pt(1)–Pt(4)–Pt(5)	58.50 (3)
Pt(2)–Pt(1)–Pt(3)	60.55 (3)	C(32)–Pt(5)–Pt(2)	97.5 (5)
Pt(2)–Pt(1)–Pt(4)	60.94 (3)	C(32)–Pt(5)–Pt(1)	83.3 (5)
Pt(2)–Pt(1)–Pt(5)	61.55 (3)	C(32)–Pt(5)–Pt(4)	40.3 (5)
Pt(3)–Pt(1)–Pt(4)	110.74 (3)	C(56)–Pt(5)–Pt(2)	167.9 (6)
Pt(3)–Pt(1)–Pt(5)	113.38 (4)	C(56)–Pt(5)–Pt(1)	125.9 (7)
Pt(4)–Pt(1)–Pt(5)	63.13 (3)	C(56)–Pt(5)–Pt(4)	134.5 (6)
C(20)–Pt(2)–Fe(1)	94.6 (6)	C(55)–pT(5)–Pt(2)	143.1 (6)
C(20)–Pt(2)–Pt(1)	146.5 (6)	C(55)–Pt(5)–Pt(1)	161.0 (6)
C(20)–Pt(2)–Pt(3)	153.8 (6)	C(55)–Pt(5)–Pt(4)	125.4 (6)
C(20)–Pt(2)–Pt(4)	89.8 (6)	C(51)–Pt(5)–Pt(2)	88.4 (5)
C(20)–Pt(2)–Pt(5)	89.0 (6)	C(51)–Pt(5)–Pt(1)	88.6 (6)
Fe(1)–Pt(2)–Pt(1)	118.90 (7)	C(51)–Pt(5)–Pt(4)	141.4 (5)
Fe(1)–Pt(2)–Pt(3)	59.16 (7)	C(52)–Pt(5)–Pt(2)	84.3 (5)
Fe(1)–Pt(2)–Pt(4)	143.65 (7)	C(52)–Pt(5)–Pt(1)	112.1 (6)
Fe(1)–Pt(2)–Pt(5)	151.87 (7)	C(52)–Pt(5)–Pt(4)	139.9 (5)
Pt(1)–Pt(2)–Pt(3)	59.78 (3)	Pt(2)–Pt(5)–Pt(1)	55.93 (3)
Pt(1)–Pt(2)–Pt(4)	62.80 (3)	Pt(2)–Pt(5)–Pt(4)	57.52 (2)
Pt(1)–Pt(2)–Pt(5)	62.52 (3)	Pt(1)–Pt(5)–Pt(4)	58.37 (2)
Pt(3)–Pt(2)–Pt(4)	111.63 (4)	C(11)–Fe(1)–Pt(2)	162.9 (7)
Pt(3)–Pt(2)–Pt(5)	113.56 (3)	C(11)–Fe(1)–Pt(3)	102.0 (7)
Pt(4)–Pt(2)–Pt(5)	64.06 (3)	C(14)–Fe(1)–Pt(2)	99.0 (8)
C(31)–Pt(3)–Fe(1)	92.2 (7)	C(14)–Fe(1)–Pt(3)	161.0 (8)
C(31)–Pt(3)–Fe(2)	91.2 (7)	C(12)–Fe(1)–Pt(2)	86.2 (6)
C(31)–Pt(3)–Pt(1)	148.8 (7)	C(12)–Fe(1)–Pt(3)	80.2 (6)
C(31)–Pt(3)–Pt(2)	150.9 (7)	C(13)–Fe(1)–Pt(2)	75.1 (8)
Fe(1)–Pt(3)–Fe(2)	176.5 (1)	C(13)–Fe(1)–Pt(3)	74.6 (7)
Fe(1)–Pt(3)–Pt(1)	118.47 (7)	Pt(2)–Fe(1)–Pt(3)	61.98 (6)
Fe(1)–Pt(3)–Pt(2)	58.85 (7)	C(23)–Fe(2)–Pt(1)	82.5 (7)
Fe(2)–Pt(3)–Pt(1)	58.08 (7)	C(23)–Fe(2)–Pt(3)	78.9 (8)
Fe(2)–Pt(3)–Pt(2)	117.68 (7)	C(24)–Fe(2)–Pt(1)	98.0 (7)
Pt(1)–Pt(3)–Pt(2)	59.67 (3)	C(24)–Fe(2)–Pt(3)	159.6 (7)
C(32)–Pt(4)–Pt(2)	99.6 (5)	C(21)–Fe(2)–Pt(1)	166.0 (7)
C(32)–Pt(4)–Pt(1)	84.2 (5)	C(21)–Fe(2)–Pt(3)	104.2 (7)
C(32)–Pt(4)–Pt(5)	41.5 (5)	C(22)–Fe(2)–Pt(1)	81.1 (6)
C(46)–Pt(4)–Pt(2)	167.8 (5)	C(22)–Fe(2)–Pt(3)	75.8 (7)
C(46)–Pt(4)–Pt(1)	124.0 (5)	Pt(1)–Fe(2)–Pt(3)	61.77 (7)
C(46)–Pt(4)–Pt(5)	133.4 (5)	O(32)–C(32)–Pt(4)	133 (1)
C(45)–Pt(4)–Pt(2)	143.6 (5)	O(32)–C(32)–Pt(5)	129 (1)
C(45)–Pt(4)–Pt(1)	160.1 (5)	Pt(4)–C(32)–Pt(5)	98.2 (9)
C(45)–Pt(4)–Pt(5)	126.6 (5)	O–C–M (av)	177 (2)

[a] Angles are in degrees. Estimated standard deviations in the least significant figure are given in parentheses.

Table IX. Positional Parameters and *B*(eq) Values for $Pt_5Fe_2(CO)_7(PhC_2Ph)_4(C_8H_{12})$ (4)

atom	*x*	*y*	*z*	*B*(eq), Å^2
Pt(1)	0.38007 (10)	0.17492 (8)	0.80895 (8)	3.27 (8)
Pt(2)	0.40996 (10)	0.31255 (8)	0.79893 (8)	3.27 (8)
Pt(3)	0.48993 (11)	0.11049 (8)	0.73764 (8)	3.42 (8)
Pt(4)	0.46367 (11)	0.34276 (8)	0.68190 (8)	3.50 (8)
Pt(5)	0.52755 (10)	0.24224 (8)	0.75436 (8)	3.32 (8)
Fe(1)	0.2626 (4)	0.2665 (3)	0.7638 (3)	3.6 (3)
Fe(2)	0.4230 (4)	0.0510 (3)	0.8191 (3)	3.7 (3)
O(11)	0.2319 (18)	0.3970 (15)	0.7014 (14)	6.6 (8)
O(12)	0.2652 (17)	0.1814 (15)	0.6541 (14)	6.3 (7)
O(13)	0.088 (2)	0.2432 (17)	0.7530 (15)	7.3 (8)
O(21)	0.374 (2)	−0.0154 (19)	0.9268 (18)	9 (1)
O(22)	0.487 (2)	−0.0738 (19)	0.7793 (18)	10 (1)
O(23)	0.268 (2)	0.0405 (16)	0.7219 (16)	7.4 (9)
O(31)	0.391 (2)	0.0863 (17)	0.6045 (18)	8 (1)
C(11)	0.247 (3)	0.343 (2)	0.7306 (20)	5 (1)
C(12)	0.270 (3)	0.217 (2)	0.703 (2)	6 (1)
C(13)	0.158 (3)	0.254 (2)	0.754 (2)	6 (1)
C(16)	0.479 (2)	0.1333 (16)	0.8671 (17)	2.8 (8)
C(17)	0.305 (2)	0.2229 (16)	0.8503 (16)	2.3 (8)
C(21)	0.389 (3)	0.012 (3)	0.887 (3)	7 (1)
C(22)	0.461 (3)	−0.020 (2)	0.794 (2)	6 (1)
C(23)	0.328 (3)	0.045 (2)	0.761 (2)	5 (1)
C(25)	0.496 (2)	0.3804 (18)	0.7744 (18)	3.4 (9)
C(31)	0.430 (3)	0.100 (3)	0.659 (3)	8 (1)
C(35)	0.589 (3)	0.144 (2)	0.6995 (20)	4 (1)
C(36)	0.535 (2)	0.1068 (17)	0.8308 (17)	3.0 (8)
C(41)	0.389 (3)	0.421 (2)	0.636 (2)	5 (1)
C(42)	0.317 (3)	0.392 (3)	0.580 (3)	8 (1)
C(43)	0.315 (4)	0.323 (3)	0.569 (3)	10 (2)
C(44)	0.403 (3)	0.285 (2)	0.596 (2)	6 (1)
C(45)	0.474 (3)	0.297 (2)	0.587 (2)	5 (1)
C(46)	0.496 (3)	0.355 (3)	0.545 (3)	9 (2)
C(47)	0.502 (3)	0.420 (2)	0.572 (2)	7 (1)
C(48)	0.466 (3)	0.436 (2)	0.6267 (20)	5 (1)
C(52)	0.544 (2)	0.3263 (18)	0.8018 (17)	3.1 (8)
C(53)	0.613 (2)	0.2057 (19)	0.7161 (18)	3.5 (9)
C(71)	0.325 (2)	0.2885 (18)	0.8534 (18)	3.1 (8)

other platinum atoms each contain one linear terminal carbonyl ligand. The Pt_5 cluster in **2** is structurally similar to those in the molecules $Pt_5(CO)_6(PPh_3)_4$ (**6**)[16] and

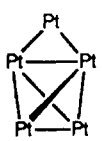

6

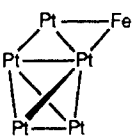

7

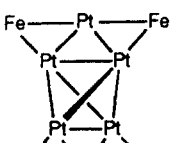

8

$Pt_5Fe(CO)_9(PEt_3)_4$ (**7**).[17] The large anion $[Pt_6Fe_4(CO)_{22}]^{2-}$ (**8**) also has important structural similarities in its Pt_6 cluster grouping and also contains four similarly positioned bridging $Fe(CO)_4$ groups.[13] The bonding in **2** can be rationalized by the resonance structures A and A′, which

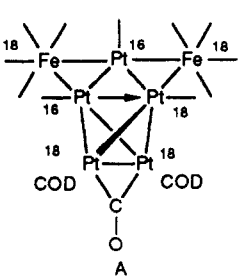

A

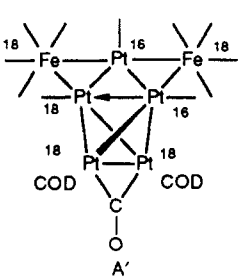

A′

(16) Bender, R.; Braunstein, P.; Fischer, J.; Ricard, L.; Mitschler, A. *Nouv. J. Chim.* **1981**, *5*, 81.
(17) Bender, R.; Braunstein, P.; Bayeul, D.; Dusausoy, Y. *Inorg. Chem.* **1989**, *28*, 2381.

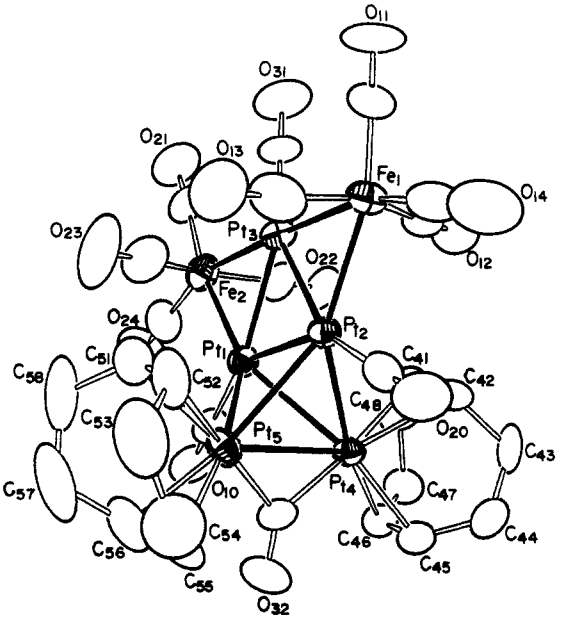

Figure 3. ORTEP drawing of $Pt_5Fe_2(CO)_{12}(COD)_2$ (**2**) showing 50% probability thermal ellipsoids.

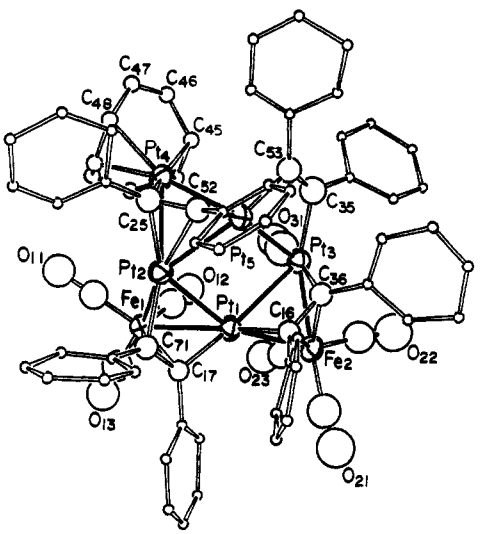

Figure 4. ORTEP drawing of $Pt_5Fe_2(CO)_7(COD)(\mu_3\text{-}PhC_2Ph)_3(\mu\text{-}PhC_2Ph)$ (**4**).

Table X. Intramolecular Distances for 4[a]

Pt(1)-C(17)	1.93 (3)	Pt(4)-Pt(5)	2.576 (2)
Pt(1)-C(16)	1.98 (3)	Pt(5)-C(52)	1.93 (4)
Pt(1)-Fe(2)	2.541 (6)	Pt(5)-C(53)	1.93 (4)
Pt(1)-Fe(1)	2.657 (6)	Fe(1)-C(12)	1.65 (5)
Pt(1)-Pt(2)	2.777 (2)	Fe(1)-C(11)	1.65 (4)
Pt(1)-Pt(3)	2.917 (2)	Fe(1)-C(13)	1.72 (5)
Pt(2)-C(71)	2.08 (4)	Fe(1)-C(71)	1.98 (4)
Pt(2)-C(25)	2.11 (4)	Fe(1)-C(17)	2.00 (3)
Pt(2)-C(52)	2.21 (4)	Fe(2)-C(22)	1.67 (5)
Pt(2)-Fe(1)	2.537 (6)	Fe(2)-C(23)	1.75 (4)
Pt(2)-Pt(5)	2.733 (2)	Fe(2)-C(21)	1.83 (5)
Pt(2)-Pt(4)	2.892 (2)	Fe(2)-C(16)	2.02 (3)
Pt(3)-C(31)	1.73 (6)	Fe(2)-C(36)	2.11 (4)
Pt(3)-C(36)	1.94 (3)	C(16)-C(36)	1.43 (4)
Pt(3)-C(35)	2.10 (4)	C(17)-C(71)	1.33 (4)
Pt(3)-Fe(2)	2.551 (6)	C(25)-C(52)	1.37 (4)
Pt(3)-Pt(5)	2.676 (2)	C(35)-C(53)	1.29 (4)
Pt(4)-C(25)	2.05 (4)	C(41)-C(48)	1.37 (5)
Pt(4)-C(41)	2.07 (4)	C(44)-C(45)	1.25 (5)
Pt(4)-C(48)	2.19 (4)	O-C (av)	1.18 (5)
Pt(4)-C(44)	2.19 (5)	Pt(1)-Pt(5)	3.223 (2)
Pt(4)-C(45)	2.26 (4)	Pt(2)-Pt(3)	4.488 (2)

[a] Distances are in angstroms. Estimated standard deviations in the least significant figure are given in parentheses.

Table XI. Intramolecular Bond Angles for 4[a]

C(17)-Pt(1)-Pt(2)	72 (1)	C(31)-Pt(3)-Fe(2)	111 (2)
C(17)-Pt(1)-Pt(3)	175 (1)	C(31)-Pt(3)-Pt(5)	108 (2)
C(16)-Pt(1)-Fe(1)	159 (1)	C(31)-Pt(3)-Pt(1)	106 (2)
C(16)-Pt(1)-Pt(2)	109 (1)	C(36)-Pt(3)-Pt(5)	83 (1)
C(16)-Pt(1)-Pt(3)	68 (1)	C(36)-Pt(3)-Pt(1)	68 (1)
Fe(2)-Pt(1)-Fe(1)	148.2 (2)	C(35)-Pt(3)-Fe(2)	156 (1)
Fe(2)-Pt(1)-Pt(2)	153.7 (2)	C(35)-Pt(3)-Pt(5)	64 (1)
Fe(2)-Pt(1)-Pt(3)	55.2 (1)	C(35)-Pt(3)-Pt(1)	134 (1)
Fe(1)-Pt(1)-Pt(2)	55.6 (1)	Fe(2)-Pt(3)-Pt(5)	118.8 (1)
Fe(1)-Pt(1)-Pt(3)	126.9 (1)	Fe(2)-Pt(3)-Pt(1)	54.9 (1)
Pt(2)-Pt(1)-Pt(3)	104.02 (7)	Pt(5)-Pt(3)-Pt(1)	70.22 (6)
C(71)-Pt(2)-C(25)	150 (1)	C(25)-Pt(4)-Pt(5)	74 (1)
C(71)-Pt(2)-C(52)	145 (1)	Pt(5)-Pt(4)-Pt(2)	59.63 (6)
C(71)-Pt(2)-Pt(5)	135 (1)	C(52)-Pt(5)-Pt(4)	69 (1)
C(71)-Pt(2)-Pt(1)	65 (1)	C(52)-Pt(5)-Pt(3)	155 (1)
C(71)-Pt(2)-Pt(4)	156 (1)	C(53)-Pt(5)-Pt(4)	106 (1)
C(25)-Pt(2)-Fe(1)	144 (1)	C(53)-Pt(5)-Pt(2)	171 (1)
C(25)-Pt(2)-Pt(5)	70 (1)	Pt(4)-Pt(5)-Pt(3)	128.27 (8)
C(25)-Pt(2)-Pt(1)	141 (1)	Pt(4)-Pt(5)-Pt(2)	65.95 (7)
C(52)-Pt(2)-Fe(1)	159 (1)	Pt(3)-Pt(5)-Pt(2)	112.16 (8)
C(52)-Pt(2)-Pt(1)	108 (1)	Pt(2)-Fe(1)-Pt(1)	64.6 (1)
Fe(1)-Pt(2)-Pt(5)	115.3 (1)	C(16)-Fe(2)-Pt(3)	76 (1)
Fe(1)-Pt(2)-Pt(1)	59.8 (1)	C(36)-Fe(2)-Pt(1)	74 (1)
Fe(1)-Pt(2)-Pt(4)	106.9 (1)	Pt(1)-Fe(2)-Pt(3)	69.9 (2)
Pt(5)-Pt(2)-Pt(1)	71.60 (6)	Pt(5)-C(52)-Pt(2)	82 (1)
Pt(5)-Pt(2)-Pt(4)	54.42 (6)	O-C-M (av)	175 (5)
Pt(1)-Pt(2)-Pt(4)	111.34 (7)		

[a] Angles are in degrees. Estimated standard deviations in the least significant figure are given in parentheses.

contain a donor/acceptor Pt–Pt bond between the atoms Pt(1) and Pt(2) and a combination of 16- and 18-electron configurations for the platinum atoms. The presence of the labile COD ligands in **2** provides a great opportunity to develop further the organic chemistry of these platinum clusters under mild conditions. Thus, the reactions of **2** with PhC≡CPh and PhC≡CH were investigated. The reaction of **2** with PhC_2Ph yielded $Pt_5Fe_2(CO)_7(COD)(\mu_3\text{-}PhC_2Ph)_3(\mu\text{-}PhC_2Ph)$ (**4**; 36%). Compound **4** was characterized by a single-crystal X-ray diffraction analysis, and an ORTEP diagram of its molecular structure is shown in Figure 4. Final positional parameters are listed in Table IX. Selected intramolecular bond distances and angles are listed in Tables X and XI. The cluster consists of a central square of four platinum atoms, Pt(1), Pt(2), Pt(3), and Pt(5), that is nearly planar. The dihedral angle between the Pt(1), Pt(2), Pt(5) and Pt(1), Pt(3), Pt(5) planes is 167°. Three edges of this square are bridged by metal atoms. The Pt(2)–Pt(5) edge contains a bridging platinum atom, Pt(4), while the Pt(1)–Pt(2) and Pt(1)–Pt(3) edges each contain a bridging $Fe(CO)_3$ group. Each of the three triangular metal groupings formed by these bridging metal atoms also contains a triply bridging PhC_2Ph ligand.

The bridging metal atoms lie significantly out of the Pt_4 plane with Pt(4) and Fe(1) on one side displaced by 1.70 and 1.65 Å, respectively, and Fe(2) on the other side displaced by 0.84 Å. The triply bridging PhC_2Ph ligands adopt the usual μ_3-$\parallel$ bonding mode. The fourth PhC_2Ph ligand is bonded to only two metal atoms, Pt(3) and Pt(5), and adopts the μ-$\parallel$ mode. This is a relatively rare occurrence for two-center alkyne bridges but was observed in the related dinuclear platinum complex $Pt_2(CO)_2(PPh_3)_2(\mu\text{-}MeO_2CC_2CO_2Me)$.[18]

The platinum–platinum bonding is irregular. The shortest Pt–Pt bond is Pt(4)–Pt(5) (2.576 (2) Å), and the longest is Pt(1)–Pt(3) (2.917 (2) Å). Platinum–platinum single bonds typically exhibit a wide range of distances, and the distances observed in **4** are not unusual. The platinum–iron distances are more regular and all lie in the range 2.537 (6)–2.657 (6) Å. Electron counting shows that both iron atoms achieve 18-electron configurations. The platinum atoms can be assigned to a combination of 16- and 18-electron counts by employing a network of donor/acceptor bonds as shown in the line structure B.

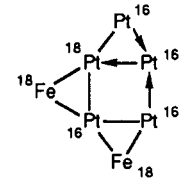

B

There appears to be much steric crowding between the alkyne ligands. The C–C vectors of C≡C bonds all have approximately perpendicular orientations that may inhibit alkyne–alkyne coupling processes. Compound **4** contains one COD ligand that is coordinated to Pt(4).

Compounds **2** and **4** both contain a total of 98 valence electrons, yet the latter compound clearly has a more open structure for the cluster. The stabilization of the open structure may be due to steric crowding effects caused by the alkyne ligands that may be too great in a closed structure.

The reaction of **2** with PhC≡CH yielded the new compound $PtFe(CO)_3(COD)[\mu\text{-}PhCC(H)C(H)CPh]$ (**5**) as the principal product (26%). An ORTEP diagram of the molecular structure of **5** is shown in Figure 5. Final positional parameters are listed in Table XII. Selected interatomic distances and angles are listed in Tables XIII and XIV. The molecule contains one platinum and one iron atom that can be regarded as bonded on the basis of their internuclear separation of 2.830 (3) Å. The metal atoms are bridged by a PhCCHCHCPh ligand formed by the coupling of two PhC_2H molecules at the less crowded, unsubstituted end of the alkyne. The ligand contains two Pt–C σ bonds, Pt–C(30) = 2.01 (2) Å and Pt–C(40) = 2.04 (2) Å, while all four carbon atoms are π-bonded to the $Fe(CO)_3$ grouping. Compound **5** is structurally very similar to the well-known ferroles or ferracyclopentadiene complexes **9** that are typically obtained from the reactions of

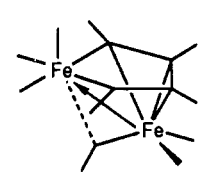

9

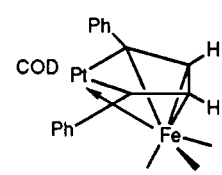

5

iron carbonyl with alkynes.[19] The Fe–Fe bond in the ferrole complexes **9** is generally regarded to be a donor/acceptor bond and invariably contains a semibridging carbonyl ligand.[20] Similarly, the Fe–Pt bond in **5** may be regarded as a donor/acceptor bond from Fe to Pt; however, although the carbonyl ligand C(11)–O(11) is suitably oriented to assume a semibridging position across the Fe–Pt bond, it shows very little tendency to do so. The Fe–C(11)–O(11) angle of 175 (2)° is not significantly less linear than that of the other carbonyl ligands bonded to the iron

(18) Koie, Y.; Shinoda, S.; Saito, Y.; Fitzgerald, B. J.; Pierpont, C. G. *Inorg. Chem.* **1980**, *19*, 770.

(19) Fehlhammer, W. B.; Stolzenberg, H. In *Comprehensive Organometallic Chemistry*; Wilkinson, G., Stone, F. G. A., Abel, E., Eds.; Pergamon: Oxford, U. K., 1982; Chapter 31.4.

(20) Cotton, F. A. *Prog. Inorg. Chem.* **1976**, *21*, 1.

Table XII. Positional Parameters and B(eq) Values for $PtFe(CO)_3(COD)[\mu$-PhCC(H)C(H)CPh] (5)

atom	x	y	z	B(eq), Å^2
Pt	0.67897 (8)	0.07139 (5)	0.83082 (6)	3.12 (3)
Fe	0.6426 (3)	0.19820 (19)	0.6892 (2)	4.0 (2)
O(11)	0.8160 (16)	0.0702 (13)	0.6400 (10)	7 (1)
O(12)	0.4564 (18)	0.2034 (15)	0.5077 (13)	9 (1)
O(13)	0.7766 (19)	0.3543 (11)	0.6484 (13)	8 (1)
C(1)	0.876 (2)	0.0187 (13)	0.8792 (15)	4.2 (5)
C(2)	0.8316 (20)	0.0276 (13)	0.9525 (14)	4.0 (5)
C(3)	0.771 (2)	−0.0392 (16)	1.0054 (17)	6.3 (7)
C(4)	0.646 (3)	−0.073 (2)	0.9602 (19)	8.7 (7)
C(5)	0.591 (2)	−0.0528 (15)	0.8588 (16)	5.5 (6)
C(6)	0.638 (2)	−0.0663 (17)	0.7875 (15)	6.0 (5)
C(7)	0.765 (3)	−0.1117 (18)	0.7942 (19)	8.2 (8)
C(8)	0.888 (2)	−0.0711 (18)	0.8380 (16)	6.4 (6)
C(11)	0.743 (2)	0.1191 (20)	0.6621 (16)	6 (2)
C(12)	0.530 (3)	0.2027 (18)	0.579 (2)	7 (2)
C(13)	0.720 (3)	0.2924 (15)	0.6653 (16)	5 (1)
C(30)	0.5108 (20)	0.1257 (14)	0.7583 (14)	4.0 (5)
C(31)	0.3848 (17)	0.0802 (14)	0.7124 (12)	3.2 (4)
C(32)	0.2796 (19)	0.0899 (13)	0.7533 (13)	4.0 (5)
C(33)	0.166 (2)	0.0443 (13)	0.7156 (15)	4.5 (5)
C(34)	0.151 (2)	−0.0079 (15)	0.6385 (16)	5.2 (6)
C(35)	0.258 (2)	−0.0143 (15)	0.5952 (16)	5.2 (6)
C(36)	0.373 (2)	0.0260 (13)	0.6323 (15)	4.5 (5)
C(37)	0.506 (2)	0.2182 (15)	0.7671 (15)	4.7 (6)
C(40)	0.7316 (19)	0.1984 (13)	0.8401 (14)	4.1 (5)
C(41)	0.8631 (18)	0.2323 (12)	0.8882 (13)	3.1 (4)
C(42)	0.972 (2)	0.2329 (13)	0.8509 (14)	4.1 (5)
C(43)	1.094 (2)	0.2619 (14)	0.9003 (15)	4.8 (5)
C(44)	1.104 (2)	0.2959 (14)	0.9862 (15)	4.9 (5)
C(45)	0.998 (2)	0.3011 (14)	1.0221 (14)	4.5 (5)
C(46)	0.8753 (20)	0.2697 (13)	0.9745 (14)	4.0 (5)
C(47)	0.623 (2)	0.2574 (14)	0.8145 (14)	4.1 (5)

Table XIII. Intramolecular Distances for 5[a]

Pt-C(30)	2.01 (2)	C(1)-C(8)	1.54 (3)
Pt-C(40)	2.04 (2)	C(2)-C(3)	1.53 (3)
Pt-C(1)	2.18 (2)	C(3)-C(4)	1.42 (3)
Pt-C(2)	2.21 (2)	C(4)-C(5)	1.50 (3)
Pt-C(5)	2.22 (2)	C(5)-C(6)	1.29 (3)
Pt-C(6)	2.24 (3)	C(6)-C(7)	1.49 (3)
Pt-Fe	2.830 (3)	C(7)-C(8)	1.44 (3)
Fe-C(11)	1.73 (3)	C(30)-C(37)	1.44 (3)
Fe-C(13)	1.75 (3)	C(30)-C(31)	1.51 (3)
Fe-C(12)	1.77 (3)	C(37)-C(47)	1.39 (3)
Fe-C(37)	2.07 (2)	C(40)-C(47)	1.44 (2)
Fe-C(47)	2.12 (2)	C(40)-C(41)	1.49 (2)
Fe-C(40)	2.20 (2)	O-C (av)	1.17 (3)
Fe-C(30)	2.22 (2)	C(Ph)-C (av)	1.39 (3)
C(1)-C(2)	1.29 (3)		

[a] Distances are in angstroms. Estimated standard deviations in the least significant figure are given in parentheses.

Table XIV. Intramolecular Bond Angles for 5[a]

C(30)-Pt-C(40)	79.7 (8)	C(11)-Fe-Pt	72.6 (8)
C(30)-Pt-C(1)	166.3 (8)	C(13)-Fe-Pt	138.1 (8)
C(30)-Pt-C(2)	158.8 (8)	C(12)-Fe-Pt	130.7 (9)
C(30)-Pt-C(5)	96.3 (8)	C(40)-Fe-C(30)	71.9 (7)
C(30)-Pt-C(6)	99.4 (8)	C(40)-Fe-Pt	45.7 (5)
C(30)-Pt-Fe	51.1 (6)	C(30)-Fe-Pt	45.0 (5)
C(40)-Pt-C(1)	96.8 (8)	Pt-C(30)-Fe	83.9 (7)
C(40)-Pt-C(2)	96.4 (8)	Pt-C(40)-Fe	83.7 (7)
C(40)-Pt-C(5)	160.6 (8)	C(37)-C(47)-C(40)	114 (2)
C(40)-Pt-C(6)	165.6 (8)	O(11)-C(11)-Fe	175 (2)
C(40)-Pt-Fe	50.6 (6)	O(12)-C(12)-Fe	178 (3)
C(1)-Pt-C(6)	80.7 (8)	O(13)-C(13)-Fe	177 (2)
C(2)-Pt-C(5)	80.5 (8)	C(Ph)-C-C (av)	120 (2)

[a] Angles are in degrees. Estimated standard deviations in the least significant figure are given in parentheses.

atom. The ^{1}H NMR spectrum of **5** in solution is consistent with the solid-state structure. Interestingly, the hydrogen atoms on the coupled alkyne ligands exhibit a significant coupling (88 Hz) to the NMR-active isotope of platinum, ^{195}Pt.

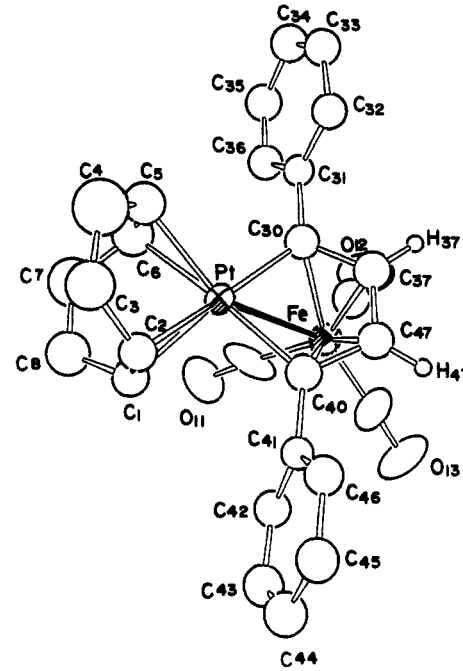

Figure 5. ORTEP drawing of $PtFe(CO)_3(COD)[\mu$-PhCC(H)C(H)CPh] (**5**) showing 50% probability thermal ellipsoids.

Scheme I

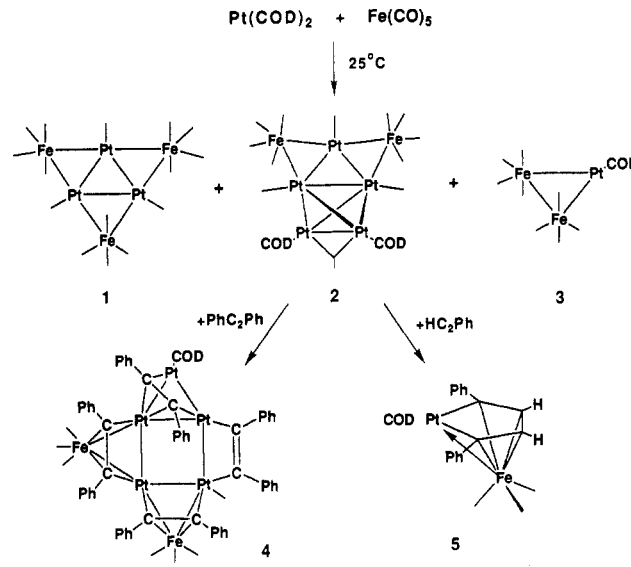

Summary

The results of this study are summarized in Scheme I. The reaction of $Fe(CO)_5$ with $Pt(COD)_2$ yielded the two new high-nuclearity cluster compounds **1** and **2** and a small amount of the previously reported compound **3**. The structures of **1** and **2** reveal a tendency of the platinum atoms to aggregate in a centralized cluster that is supported by bridging $Fe(CO)_4$ groupings. Compound **2** contains two COD ligands. Since these ligands can usually be removed easily by other reagents, reactions of **2** with PhC_2Ph and HC_2Ph were attempted. These led to the formation of compounds **4** and **5**, respectively. The addition of four PhC_2Ph ligands to **2** produced a significant opening of the metal cluster, but no alkyne coupling processes were observed. It is believed that steric effects may be at least partially responsible for this, even though the tetraphenyl-substituted ferrole derivative of **9** is known.[21]

In the formation of **5**, alkyne coupling did occur at the less crowded, unsubstituted carbon atoms, but unfortunately, the reaction was accompanied by degradation of the cluster.

Compounds **3-5** also contain COD ligands. It seems likely that these compounds should permit further study of the heteronuclear iron-platinum center. Further studies are in progress.

(21) Riley, P. E.; Davis, R. E. *Acta Crystallogr.* 1975, *B31*, 2928.

Acknowledgment. This research was supported by the National Science Foundation under Grant CHE-8919786. We wish to thank Professor C. Mealli for making the results of his studies available to us prior to publication.

Supplementary Material Available: Tables of hydrogen atom coordinates for **2** and **5**, hydrogen and ring carbon coordinates for **4**, and anisotropic thermal parameters for **1**, **2**, **4**, and **5** (16 pages); tables of structure factor amplitudes for **1**, **2**, **4**, and **5** (69 pages). Ordering information is given on any current masthead page.

Synthetic, Structural, and Bonding Studies of Phosphido-Bridged Early-Late Transition-Metal Heterobimetallic Complexes

R. Thomas Baker* and William C. Fultz

Central Research and Development Department,† Experimental Station, E. I. du Pont de Nemours and Co., Wilmington, Delaware 19880-0328

Todd B. Marder* and Ian D. Williams*

Guelph-Waterloo Centre for Graduate Work in Chemistry, Department of Chemistry, University of Waterloo, Waterloo, Ontario, Canada N2L 3G1

Received February 7, 1990

The mononuclear terminal phosphide complexes $Cp_2M(PR_2)_2$ (M = Zr, Hf; R = Et, Ph, Cy) are shown to act as chelating bis(phosphine) ligands to Ni, Pd, and Pt (M') in compounds of the form $Cp_2M(\mu\text{-}PR_2)_2M'L_n$ (n = 1, 2) and $\{Cp_2M(\mu\text{-}PR_2)_2\}_2M'$. Reaction of $Cp_2M(PEt_2)_2$ with $Ni(1,5\text{-}COD)_2$ yields either $Cp_2M(\mu\text{-}PEt_2)_2Ni(1,5\text{-}COD)$ or $\{Cp_2M(\mu\text{-}PEt_2)_2\}_2Ni$ depending on the stoichiometry employed. Analogous reactions with $Pd(PPh_3)_4$ and $Pt(PPh_3)_3$ yield mixtures of $Cp_2M(\mu\text{-}PEt_2)_2M'(PPh_3)$ and $\{Cp_2M(\mu\text{-}PEt_2)_2\}_2M'$ (M' = Pd, Pt) when the M/M' ratio is <2. With bulkier substituents, $Cp_2M(PR_2)_2$ (R = Ph, Cy) react with $Pt(1,5\text{-}COD)_2$ and $CpPd(\eta\text{-}2\text{-}Me\text{-}allyl)$ in the presence of phosphines and phosphites yielding only $Cp_2M(\mu\text{-}PR_2)_2M'L$ (L = PR'_3, $P(OR')_3$). The $M'L_2$ complexes $Cp_2M(\mu\text{-}PPh_2)_2M'(DMPE)$ were also prepared. The three classes of compounds were characterized by X-ray crystallography. The structure of $Cp_2Zr(\mu\text{-}PEt_2)_2Ni(\mu\text{-}PEt_2)_2HfCp_2$ ($C2/c$, Z = 8, a = 34.823 (4), b = 10.991 (2), c = 21.606 (3) Å, β = 105.65 (1)°) consists of two 16-e⁻ d^0 metal centers coupled to a pseudotetrahedral 18-e⁻ d^{10} Ni center by PEt_2 bridges. The MP_2Ni rings are nearly planar with an average M···Ni separation of 3.027 (1) Å. The structure of $Cp_2Hf(\mu\text{-}PPh_2)_2Pd(PPh_3)$ ($C2/c$, Z = 8, a = 27.701 (8), b = 10.654 (5), c = 30.330 (11) Å, β = 103.16 (5)°) consists of edge-shared, 16-e⁻ pseudotetrahedral Hf(IV) and trigonal planar Pd(0) centers with a puckered HfP_2Pd ring and a Hf···Pd separation of 2.896 (1) Å. In the structure of $Cp_2Hf(\mu\text{-}PPh_2)_2Pd(DMPE)$ ($C2/c$, Z = 8, a = 25.361 (12), b = 19.584 (5), c = 18.814 (13) Å, β = 126.15 (5)°) the 16-e⁻ Hf(IV) and 18-e⁻ Pd(0) centers are pseudotetrahedral, the HfP_2Pd ring is puckered and the Hf···Pd separation is 2.983 (1) Å. Extended Hückel molecular orbital calculations performed on the model complexes $Cp_2Zr(\mu\text{-}PH_2)_2M'L_n$ ($M'L_n$ = $Pt(PH_3)$, Pt(DMPE), $Rh(\eta^5\text{-indenyl})$, $Ni(\mu\text{-}PH_2)_2ZrCp_2$, and $Mo(CO)_4$) indicate the presence of M' → Zr donor-acceptor metal-metal bonds that become weaker along the series. The calculations also predict low barriers to MP_2M' ring inversion for the Pt complexes, consistent with low-temperature ^1H and ^{31}P NMR spectroscopic observations.

Introduction

Diorganophosphide $(PR_2)^-$ ligands have been widely used as bridging groups in transition-metal chemistry[1] due to the ease with which steric and electronic factors can be tuned. In bis$(PR_2)^-$-bridged complexes that have been structurally characterized,[2,3] the M-P-M' angles and M-M' distances range from 54 to 104° and 2.21 (multiple M-M bond) to 3.70 Å (M-M nonbonding), respectively, also indicating the flexibility of $(\mu\text{-}PR_2)$ groups.

As part of an extensive study of early-transition-metal complexes containing terminal $(PR_2)^-$ ligands,[4-6] we have prepared and structurally characterized[4a] $Cp_2Hf(PEt_2)_2$. This contains both planar and pyramidal phosphido groups

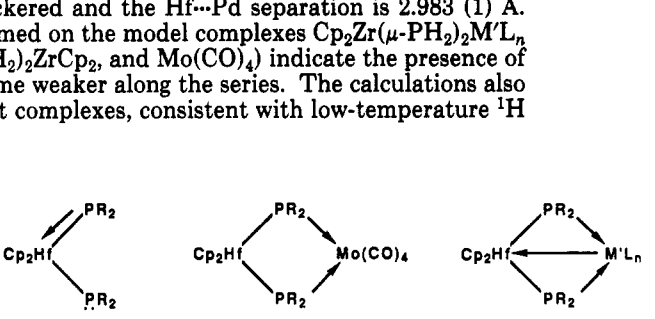

consistent with electronic structure (A) in which the Hf center is saturated. Subsequently, we demonstrated[7] the ability of $Cp_2Hf(PEt_2)_2$ to function as a bidentate phosphine ligand in $Cp_2Hf(\mu\text{-}PEt_2)_2Mo(CO)_4$ in which the Hf-Mo distance is 3.400 (1) Å. Spectroscopic properties of the heterobimetallic complex suggest that there is no significant perturbation of the $Mo(CO)_4$ unit due to interaction with the Hf, which is now electronically unsat-

† Contribution No. 4832.

0276-7333/90/2309-2357$02.50/0